



Towards Model-Informed Precision Dosing of Voriconazole: Challenging Published Voriconazole Nonlinear Mixed-Effects Models with Real-World Clinical Data

Franziska Kluwe^{1,2} · Robin Michelet¹ · Wilhelm Huisinga³ · Markus Zeitlinger⁴ · Gerd Mikus^{1,5} · Charlotte Kloft¹

Accepted: 18 May 2023 / Published online: 21 August 2023
© The Author(s) 2023

Abstract

Background and Objectives Model-informed precision dosing (MIPD) frequently uses nonlinear mixed-effects (NLME) models to predict and optimize therapy outcomes based on patient characteristics and therapeutic drug monitoring data. MIPD is indicated for compounds with narrow therapeutic range and complex pharmacokinetics (PK), such as voriconazole, a broad-spectrum antifungal drug for prevention and treatment of invasive fungal infections. To provide guidance and recommendations for evidence-based application of MIPD for voriconazole, this work aimed to (i) externally evaluate and compare the predictive performance of a published so-called ‘hybrid’ model for MIPD (an aggregate model comprising features and prior information from six previously published NLME models) versus two ‘standard’ NLME models of voriconazole, and (ii) investigate strategies and illustrate the clinical impact of Bayesian forecasting for voriconazole.

Methods A workflow for external evaluation and application of MIPD for voriconazole was implemented. Published voriconazole NLME models were externally evaluated using a comprehensive in-house clinical database comprising nine voriconazole studies and prediction-/simulation-based diagnostics. The NLME models were applied using different Bayesian forecasting strategies to assess the influence of prior observations on model predictivity.

Results The overall best predictive performance was obtained using the aggregate model. However, all NLME models showed only modest predictive performance, suggesting that (i) important PK processes were not sufficiently implemented in the structural submodels, (ii) sources of interindividual variability were not entirely captured, and (iii) interoccasion variability was not adequately accounted for. Predictive performance substantially improved by including the most recent voriconazole observations in MIPD.

Conclusion Our results highlight the potential clinical impact of MIPD for voriconazole and indicate the need for a comprehensive (pre-)clinical database as basis for model development and careful external model evaluation for compounds with complex PK before their successful use in MIPD.

1 Introduction

Model-informed precision dosing (MIPD) is an emerging approach fostering the use of mathematical models in the framework of quantitative dosing decision support. This approach aims to predict, individualize, and thereby optimize dosing and therapy outcomes based on patient characteristics and data from therapeutic drug/biomarker monitoring (TDM) [1, 2]. MIPD offers the opportunity to significantly improve the efficacy and safety of drug therapies, reduce the emergence of resistance, and save costs.

In brief, based on (preferably rich) pharmacokinetic (PK) and/or pharmacodynamic (PD) individual-level data, typically a nonlinear mixed-effects (NLME) model is developed, and the typical population PK and/or PD parameters are estimated. Different sources of variability between/within individuals are quantified and accounted for (e.g., interindividual, interoccasion, interstudy, or residual variability). Individual-specific factors (‘covariates’, e.g., *CYP2C19* genotype or body weight) can be integrated to explain part of the variability. In the clinical setting, the values of the population parameters of the developed NLME model can be used as Bayesian uncertainty priors, if available, in combination with recorded patient-specific factors, to a priori predict the exposure likely to result from a hypothetical dosing

Extended author information available on the last page of the article

Key Points

Model-informed precision dosing (MIPD) is indicated for compounds with narrow therapeutic range and complex pharmacokinetics (PK) such as voriconazole.

To guide evidence-based application of MIPD for voriconazole, a workflow for external evaluation and application of MIPD was implemented and it was shown that the aggregate model of voriconazole had a better predictive performance than the ‘standard’ nonlinear mixed-effects models but no evaluated published models were able to adequately describe the highly variable PK (especially after oral administration), indicating the need for more (semi-)mechanistic models combining in vitro and in vivo data to characterize the complex PK behavior for successful implementation of MIPD.

The clinical need for MIPD was demonstrated by high intra- and interindividual variability and low PK target attainment after standard dosing, and simulations for a representative patient illustrated how a MIPD workflow could be designed to improve target attainment. Predictive performance substantially improved by including the most recent voriconazole observations in MIPD.

regimen and thereby derive an adequate individual first dosing regimen (probabilistic setting). In combination with patient’s individual dosing history and drug monitoring data, individual parameters can be estimated (maximum a posteriori [MAP] Bayesian estimates). Thereby future trajectories of the individual concentration-time profiles will accurately be predicted and dosing regimens to achieve a desired efficacy or safety threshold be suggested (Bayesian forecasting setting). Prior to its application in MIPD, a candidate NLME model needs to be carefully selected, thoroughly evaluated, and must provide adequate predictive performance. Using external evaluation techniques, i.e., based on the candidate NLME model together with an external evaluation dataset, the predictive performance can be assessed using prediction-/simulation-based methods and retrospective application of Bayesian forecasting [2]. Candidate drugs for MIPD need to fulfill several criteria to be eligible for MIPD [1–4], all of which are met by the second-generation triazole voriconazole, classified as ‘essential medicine’ by the WHO [5]: high interindividual PK variability (e.g., metabolized by polymorphic enzymes), narrow therapeutic range, potential for severe adverse drug reactions, vulnerable patient population (e.g., pediatrics, patients undergoing transplantation), and defined relationship between dose, plasma concentration and clinical response as well as safety [6–8]. Voriconazole is commonly used for first-line treatment of invasive fungal

infections [9], and as primary or secondary prophylaxis in immunocompromised patients [10, 11]. Voriconazole PK is characterized by nonlinearity and high inter-/intraindividual variability. Potential sources of variability comprise, e.g., status of metabolizing enzymes (fraction metabolized = 98% of parent compound, primarily via polymorphic CYP2C19, 3A4 and potentially 2C9), age, sex, liver or disease status, concomitant medication, and route of administration [12–20]. The relative contribution of CYP2C19, 3A4 and 2C9 to voriconazole clearance, the (auto-) inhibitory potential of the parent compound and metabolites, as well as the mechanism of the inhibition processes were intensively discussed and only recently comprehensively investigated in systematic and quantitative in vitro investigations [21–24]. The mean contribution of the individual isoenzymes to voriconazole *N*-oxide formation was 63.1% for CYP2C19, 13.2% for CYP2C9 and 29.5% for CYP3A4. Voriconazole *N*-oxide was the weakest and voriconazole and hydroxy-voriconazole comparably strong inhibitors of CYP2C9 and CYP3A4. CYP2C19 was significantly inhibited by voriconazole only. Time-independent (i.e., competitive and non-competitive) inhibition by voriconazole, voriconazole *N*-oxide and hydroxy-voriconazole was demonstrated. Voriconazole is approved to be administered as (total body) weight-adapted intravenous (IV) infusion or orally (PO) without weight adaptation (oral bioavailability of 96% reported) [25, 26]. Polymorphic CYP2C19 and corresponding genotype-predicted phenotypes significantly impact voriconazole exposure (4-fold higher area under the concentration-time curve during one dosing interval (AUC_{τ}) in poor than in normal metabolizers) [27, 28]. Frequently used target ranges in clinical practice for minimum plasma concentrations (C_{\min} after 12 h) range from ≥ 1.0 mg/L up to 6.0 mg/L for effective and safe therapy, respectively [8, 29, 30]. Since its approval in the early 2000s, several voriconazole NLME models have been published and reviewed [21, 31], and externally evaluated [32–34]. Moreover, a so-called ‘hybrid’ (aggregate) model comprising features and prior information from six previously published NLME models including nonlinear, concentration-, CYP2C19- and time-dependent elimination has been developed for MIPD (see Section 1.1 in Online Resource 1) [35]. This work aimed to provide guidance and recommendations for evidence-based application of MIPD for the model compound voriconazole by implementing a workflow for external evaluation and application of MIPD [36]. The workflow consisted of (i) externally evaluating and comparing the predictive performance of the aggregate model, versus two ‘standard’ NLME models with linear elimination (accounting [13] or not accounting [6] for *CYP2C19* genotype), using data from a rich in-house database, and (ii) investigating different strategies and illustrating the clinical impact of Bayesian forecasting (Fig. 1).

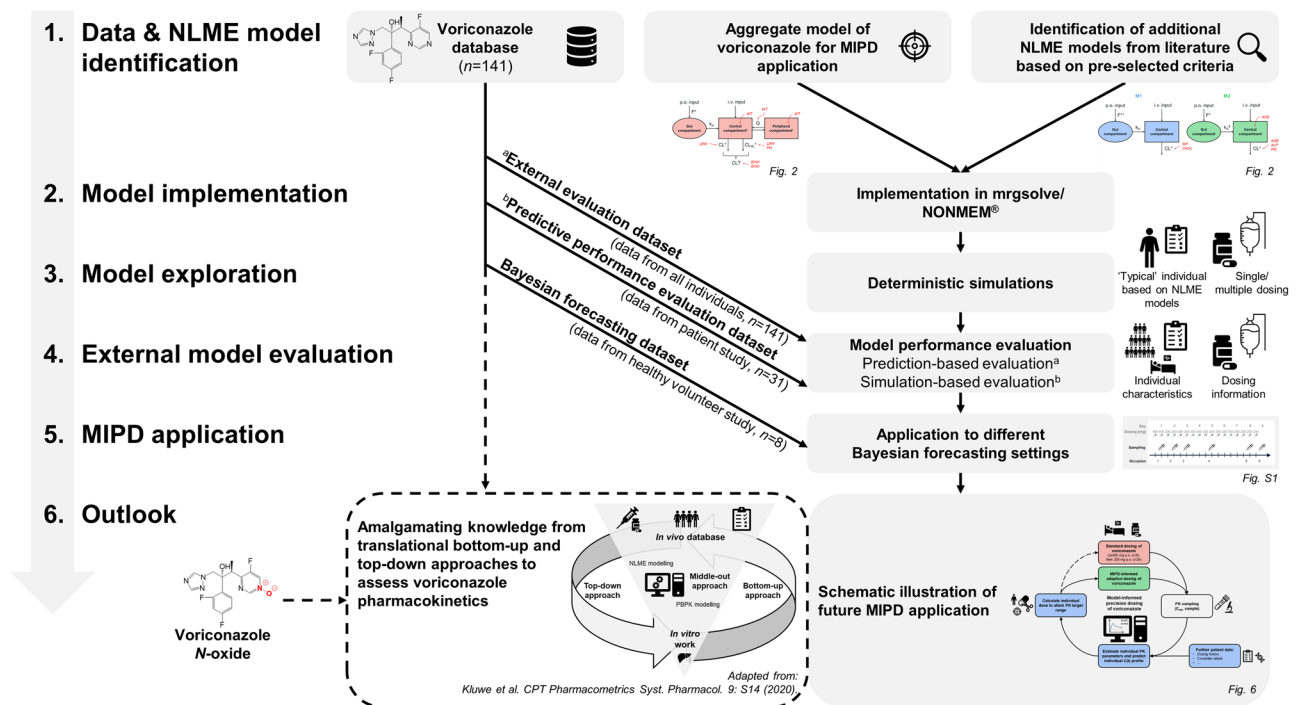


Fig. 1 Schematic workflow of the external model evaluation framework. *MIPD* model-informed precision dosing, *NLME* nonlinear mixed-effects

2 Materials and Methods

2.1 Clinical Database for Voriconazole

The in-house database for voriconazole comprised data from nine clinical voriconazole studies. Individual demographic and clinical data were acquired independently at two study sites (Department of Clinical Pharmacology, Medical University of Vienna, Austria; Department of Clinical Pharmacology and Pharmacoepidemiology, University Hospital Heidelberg, Germany). Further information on dosing, PK sampling, bioanalytical methods and genotyping are available from the respective references in Table 1. Subsets of the in-house clinical database were selected according to the most informative dosing and sampling schedules for each investigated scenario described in the following sections (Fig. 1). If covariates were missing for individuals in the clinical database, the median value of the covariate in the clinical database was imputed. Covariates that were included in the selected NLME models but not available in the clinical database were set to the reference value of the population used for model development for all evaluations and simulations. As the selected NLME models and respective parameter values were based on total plasma concentrations, *unbound* plasma concentrations in one study were transformed to *total* plasma concentrations using experimentally

determined plasma protein binding (47.1%) in the study [37].

2.2 Identification and Implementation of Nonlinear Mixed-Effects Pharmacokinetic Models of Voriconazole

The model development of the aggregate model is briefly described in Section 1.1 of Online Resource 1, for more details see [35]. To compare the performance of the aggregate model with ‘standard’ NLME models for voriconazole, a knowledge-based preselection approach was used. In addition to the aggregate model, two ‘standard’ NLME models describing the PK of voriconazole meeting the following criteria were identified from the literature (pubmed.gov): (i) parametric NLME model, (ii) all relevant parameters values published, and (iii) structural model including linear elimination, either accounting (model M1) [13] or not accounting for *CYP2C19* genotype (model M2) [6] (Fig. 2a, upper panels, Table 2). Crucial characteristics of the study populations used for model development were required to match the population characteristics of the clinical database (e.g., exclusion of patients with obesity or transplantation, pediatric patients) and route of administration (i.e., IV and PO single/multiple dosing). The identified NLME models were extracted from the literature by two independent reviewers and fixed- and random-effects parameters were

Table 1 Characteristics of clinical voriconazole database comprising nine prospective clinical studies assessing voriconazole pharmacokinetics

	Study 1	Study 2	Study 3	Study 4	Study 5	Study 6	Study 7	Study 8	Study 9
Study design	Prospective	Prospective	Prospective	Prospective	Prospective	Prospective	Prospective	Prospective	Prospective
References	[37]	[67]	[66]	[94]	[43]	[95]	[96]	[45]	[97]
Study population	Healthy volunteers	Healthy volunteers	Healthy volunteers	Healthy volunteers	Hospitalized patients	Healthy volunteers	Healthy volunteers	Healthy volunteers	Healthy volunteers
Number of individuals	10	12	15	20	31	20	17	8	8
Voriconazole dosing	Single/multiple	Single	Single	Single	Single/multiple	Single	Single	Single/multiple	Single
Voriconazole dosing regimens	2 × 6 mg/kg IV q12h, 2 × 4 mg/kg IV q12h, 3 × 200 mg PO q12h	100 mg IV, 400 mg IV	50 mg IV/PO, 400 mg IV/PO	400 mg IV/PO	2 × 400 mg PO q12h, 200 mg PO q12h	400 mg PO	400 mg PO	2 × 400 mg PO q12h, 15 × 200 mg PO q12h	400 mg IV/PO
Study visits	7	4	4	2	1 or 2	2	3	6	1
Sampling schedule ^{a,b}	Dense and sparse	Dense	Dense	Dense	Dense	Dense	Dense	Dense and sparse	Dense
Analytical method	HPLC–UV/VIS	HPLC–MS/MS	HPLC–MS/MS	HPLC–MS/MS	HPLC–MS/MS	HPLC–MS/MS	HPLC–MS/MS	HPLC–MS/MS	HPLC–MS/MS
Lower limit of quantification [mg/L]	0.15	0.0006	0.001	0.05	0.02	0.05	0.05	0.03	0.003
Continuous covariates, [unit] median (range)									
Age [years]	28.0 (21.0–46.0)	30.0 (23.0–52.0)	28.0 (22.0–52.0)	25.0 (20.0–38.0)	57.0 (20.0–72.0)	25.0 (19.0–37.0)	27.0 (22.0–35.0)	29.5 (22.0–36.0)	31.0 (24.0–46.0)
Total body weight [kg]	75.2 (65.1–83.1)	82.4 (64.0–96.0)	70.3 (55.1–96.3)	70.6 (58.0–103)	75.0 (50.0–124)	74.0 (47.0–85.0)	80.0 (68.0–93.0)	82.5 (59.3–88.0)	78.0 (55.3–89.5)
Categorical covariates, [%]									
Male	100	91.7	73.3	60.0	54.8	65.0	100	75.0	50.0
gCYP2C19 phenotype frequency ^c	10.1/30.0/10.0/10.0/–/40.0	–/16.7/41.7/25.0/16.7	–/26.7/20.0/40.0/13.3	20.0/40.0/10.0/30.0/–	–/22.6/48.4/29.0/–	15.0/45.0/25.0/15.0/–	11.8/35.3/23.5/29.4/–/47.1	–/–/–/–/–	–/–/–/–/–
gPM/gIM/gNM/gRM/gUM/NA									

gPM poor metabolizer (CYP2C19*2/*2, CYP2C19*3/*3, CYP2C19*2/*3), gIM intermediate metabolizer (CYP2C19*1/*3, CYP2C19*2/*17, CYP2C19*2/*2/*17); gNM normal metabolizer (CYP2C19*1/*1), also EM (extensive metabolizer), gRM rapid metabolizer (CYP2C19*1/*17), gUM ultrarapid metabolizer (CYP2C19*17/*17); HPLC: high-performance liquid chromatography, NA not available, NR not reported, MS mass spectrometry, PK pharmacokinetics, UV/VIS ultraviolet–visible spectrometry

^aDense: full pharmacokinetic profile

^bSparse: sampling around maximum plasma concentration and/or before the next dose (minimum plasma concentration sample)

^cGenotype-predicted CYP2C19 phenotype

fixed to reported values (see 1.1–1.2 in Online Resource 1, Table S1; model codes in Online Resource 2). The NLME models were implemented in NONMEM[®]-readable format according to the specifications given in the original publications. Critical or ambiguous aspects and interpretations of the publications were discussed and solved together with the corresponding authors.

2.3 External Model Evaluation Framework

First, to explore the NLME models and their features, deterministic simulations were performed. To evaluate the global fit and predictive performance of the models, prediction- and simulation-based diagnostics were used together with the ‘external evaluation dataset’ or subsets thereof (Fig. 1, see 1.3 in Online Resource 1). Interoccasion variability was

Table 2 Respective study and model characteristics underlying published nonlinear mixed-effects pharmacokinetic models for voriconazole [6, 13, 35], all values reported as in publications

	Aggregate model	Model 1 (M1)	Model 2 (M2)
Study design	Meta-analysis of six published population PK models	Prospective	Prospective
Number of study participants	800 (pooled)	55	151
Study population	Healthy adults ($n = 119$), patients with invasive fungal infections ($n = 426$), patients with lung/liver transplant or malignancy ($n = 35$), pediatrics ($n = 194$), adolescents ($n = 26$)	Patients with invasive fungal infections	Patients with invasive fungal infections
Voriconazole dosing	Approved dosing regimen	Approved dosing regimen	Approved dosing regimen
Study visits, median (range)	NA	3 (1–9)	NR
Samples	> 10,742 (pooled)	505	406
Samples per patient, median (range)	NR	8 (1–47)	NR
Sampling schedule ^{a,b} (number of patients)	Dense (NR), sparse (NR)	Dense (35), sparse (20)	Dense (7), sparse (144)
Continuous covariates, [unit] median (range)			
Age [years]	NR (2–99)	58 (23–78)	61 (18–99)
Total body weight [kg]	NR (10–125)	68 (42–125)	59.1 ± 7.8 (35.0–80.0) ^c
Alkaline phosphatase [U/L]	NR	NR	104 (2.0–693.0)
Categorical covariates, [%]			
Male	NR	71.0	68.9
gCYP2C19 phenotype frequency ^d (gPM/gIM/gNM/gUM)	NR	NR	12.6/43.0/42.4/1.99
Omeprazole coadministration	NR	29.1	58.9
Dexamethasone coadministration	NR	NR	59.6
Rifampicin coadministration	NR	NR	NR
Grade 3 cholestasis	NR	12.7	NR
Model	NLME PK (aggregate model)	NLME PK	NLME PK
Structural model	2-compartment model with parallel linear and nonlinear elimination	1-compartment model with linear elimination	1-compartment model with linear elimination
Identified covariates	Total body weight (allometric scaling), lean body weight, CYP2C19 gPM, CYP enzyme inhibitor/inducer	Rifampicin coadministration, severe hepatic cholestasis	Age, alkaline phosphatase, CYP2C19 gPM

NLME nonlinear mixed-effects, PK pharmacokinetics, gPM poor metabolizer ($CYP2C19^{*2/*2}$, $CYP2C19^{*3/*3}$, $CYP2C19^{*2/*3}$), gIM intermediate metabolizer ($CYP2C19^{*1/*2}$, $CYP2C19^{*1/*3}$), gNM normal metabolizer ($CYP2C19^{*1/*1}$), also EM (extensive metabolizer), gUM ultrarapid metabolizer ($CYP2C19^{*17/*17}$), NR not reported

^aDense: full pharmacokinetic profile

^bSparse: sampling before next dose (minimum plasma concentration sample)

^cMean ± standard deviation (range)

^dCYP2C19 genotype-predicted phenotype

included in the estimation of individual PK parameters but excluded for Bayesian forecasting [38, 39].

2.3.1 Deterministic Simulations

The typical concentration-time profiles of a typical patient (aged 60 years, 67 kg patient [lean body weight 54 kg] and *CYP2C19**1/*1 genotype [normal metabolizer, wild type], without co-medication) were simulated with all three models for IV and PO single doses of 400 mg over 12 h (SD1 and 2, respectively), and for different IV and PO multiple dosing regimens over 14 days with loading doses (MD1: 2×6 mg/kg IV q12 h, then 4 mg/kg IV q12 h; MD3: 2×400 mg PO, q12 h, then 200 mg PO q12 h) or without these (MD2: 4 mg/kg IV q12 h; MD4: 200 mg PO q12 h).

2.3.2 Model Performance Evaluation

To evaluate the performance of an a priori prediction, the voriconazole plasma concentrations up to 12 hours after last dose in all individuals ('external evaluation dataset', $n = 141$) were predicted using dosing information and individual covariate values and compared to the observed values (Fig. 1). For graphical model evaluation, goodness-of-prediction plots (population-predicted concentrations vs observed concentrations) were used. For numerical model evaluation, relative prediction error (PE, %), relative mean prediction error (MPE, %), and relative root mean squared error (RMSE, %) were calculated to assess bias and accuracy (Eqs. 1–3):

$$PE_i(\%) = \left(\frac{C_{\text{pred},i} - C_{\text{obs},i}}{C_{\text{obs},i}} \right) \cdot 100, \quad (1)$$

$$MPE(\%) = \frac{1}{N} \sum_{i=1}^N PE_i, \quad (2)$$

$$RMSE(\%) = \sqrt{\frac{1}{N} \sum_{i=1}^N PE_i^2}, \quad (3)$$

where N denotes the number of observations. Predictive performance of all models was further assessed using simulation-based diagnostics, i.e., prediction-corrected visual predictive checks (pcVPC) [40], normalized prediction discrepancies (NPD) and normalized prediction distribution errors (NPDE) [41, 42]. Therefore, a subset of the external evaluation dataset ('predictive performance evaluation dataset', $n = 31$) comprising real-world clinical data of 31 patients was used [43], including individual patient's dosing history and covariate information (Fig. 1). For pcVPC and

NPD/NPDE, 1000 and 2000 Monte-Carlo simulations were performed, respectively (see 1.3.1 in Online Resource 1).

2.3.3 Bayesian Forecasting

To investigate different strategies within a Bayesian forecasting setting [44] and to assess the influence of prior observations on model predictivity, a subset of the external evaluation dataset ('Bayesian forecasting dataset', $n = 8$) was used comprising eight individuals in whom voriconazole concentrations across six occasions (i.e., dosing interval with observed voriconazole concentration) were available (Fig. S1) [45]. The individual predicted voriconazole concentrations of the 'most recent' (i.e., 6th) occasion were forecasted by covariate information only (a priori prediction) and, in strategy (a), using the first one, two, three, four, or five prior observations (i.e., one observation per occasion), or in strategy (b), using different combinations of up to three prior observations (Fig. S2). The impact of number and timing of prior observations on the predictive performance was assessed using individual PE, relative MPE, and RMSE.

2.4 Clinical Impact of Bayesian Forecasting

To illustrate the clinical impact of Bayesian forecasting, a representative patient (based on the characteristics of the 'predictive performance evaluation dataset') receiving the standard multiple dosing regimen (MD3) was simulated using the aggregate model. Based on a C_{min} sample (when $C_{\text{min}} < 1.0$ mg/L) taken before administration of the 6th dose (end of Day 3), patient-individual PK parameters were estimated, future trajectories of the individual concentration-time profile predicted for maintenance dosing of 200 (standard), 250, 300, 350 and 400 mg, and dose adaptations proposed to attain therapeutic concentrations. For illustrative purposes, a simplified approach was used that did not account for variability or uncertainty in the PK parameters, the predicted exposure, or the PK target threshold.

2.5 Software

Dataset development, exploratory statistical and graphical data analyses as well as post-processing of NONMEM[®] output were performed using R 3.6.0 (R Foundation for Statistical Computing, Austria), along with RStudio[®] 1.2.1335 (RStudio, Inc., USA). For external model evaluation and simulations, NONMEM[®] 7.4.3 with MAXEVAL=0 option (Icon Development Solutions, USA) [46] in conjunction with PsN 4.8.1 (Uppsala University, Sweden) [47], Pirana 2.9.6 (Pirana Software & Consulting BV, Netherlands) [48], R packages xpose4 4.6.1 (Uppsala University, Sweden) [49, 50], mrgsolve 0.10.0 (Metrum Research Group LLC, USA)

[51], and NPDE 3.1 (INSERM, National Institute of Health and Medical Research, France) [52] were used.

3 Results

The schematic workflow of the external model evaluation framework comprising deterministic simulations, prediction-/simulation-based model performance evaluation and different strategies for Bayesian forecasting is illustrated in Fig. 1.

3.1 External Evaluation Datasets

The clinical database consisted of 141 individuals (71.6% male, 22.0% hospitalized patients). The primary indication for the hospitalized patients receiving voriconazole as pre-emptive treatment of probable fungal infection were hematological diseases (e.g., multiple myeloma) and acute myeloid leukemia. Study designs varied from single dosing, cross-over designs with wash-out periods, to multiple-dosing studies. Total voriconazole plasma concentrations up to 12 h after administration following dense/sparse sampling schedules obtained after single/multiple subtherapeutic/clinical doses following IV/PO administration in healthy volunteers and hospitalized patients, covering a broad spectrum of covariates (e.g., sex, age, weight, *CYP2C19* genotype), with and without comedication, were included in the external evaluation dataset (Table 1). Information on *CYP2C19* genotype was missing for 19 individuals and the most prevalent genotype was imputed for these individuals (*CYP2C19**1/*1, wild type). A total of 5405 PK samples that were collected after 486 administered doses were available. Only 1.31% were below the lower limit of quantification and excluded, hence 5334 samples were retained in the 'external evaluation dataset' for predictive performance assessment.

3.2 External Model Evaluation

The simulated voriconazole plasma concentration-time profiles of a 'typical patient' after single administration of 400 mg differed markedly between all models, especially after IV infusion (Fig. 2b). Simulated maximum concentrations (C_{\max}) after 400 mg IV administration (SD1) varied 2-fold (1.95 [M2], 4.11 mg/L [M1]). Simulated $C_{\min,24h}$ also varied considerably (~ 7-fold) between 0.11 mg/L (aggregate model) and 0.74 mg/L (M1). Reported oral bioavailability of voriconazole ranged between 63.0% (M1) and 89.5% (M2), and simulated C_{\max} after oral (SD2, 1.6 mg/mL [M2] to 2.33 mg/L [M1]) was lower than after IV administration (SD1) with time to reach C_{\max} of approximately 1.25 h (aggregate

model) to 2.75 h (M1). The $C_{\min,12h}$ target threshold for efficacy of 1 mg/L was predicted to be reached after IV and PO administration of 400 mg using models M1 and M2, but not using the aggregate model. After IV administration (400 mg, Fig. 2c), total voriconazole clearance substantially differed ranging from 5.20 L/h (M1, constant) to 15.9 L/h (aggregate model, around 2 h after administration, decreasing from initial 81.9 L/h).

Deterministic simulations of IV and PO multiple-dosing regimens (Fig. 2d) showed that (i) as expected, steady state was reached earlier when administering loading-dose regimens (MD1, MD3), (ii) using models M1 and M2, the PK target threshold for efficacy was already attained after single dosing when administering loading-dose regimens (MD1, MD3), and (iii) using the aggregate model, the PK target threshold for efficacy was not attained using PO dosing regimens MD3 or MD4. The $C_{\min,12h}$ target threshold for safety was never exceeded.

The predictive performance of the a priori predicted voriconazole concentrations was highly variable, as can be seen from the graphical analysis of goodness-of-prediction plots (Fig. 3), but overall best for the aggregate model. Graphical results were closely mirrored in numerical estimates of the model predictive performance (Table 3), indicating the best predictive performance for the aggregate model. Mean prediction error ranged from 36.7% (95% CI 24.9, 48.4) to 151% (95% CI 137, 164) for the aggregate model and M1, respectively, and RMSE from 429 to 524% for M2 and M1, respectively. For all models, MPE and RMSE were significantly higher after PO than after IV administration, indicating a low predictive performance for oral administration.

As shown by the simulation-based diagnostics, the predictive performance of the models was highly variable and model misspecification describing absorption was evident for all models, which was expected for models M1 and M2 due to the sparse PK sampling but not for the aggregate model (Fig. 4 showing 50th [median], 5th and 95th percentiles, including 95% CIs, obtained from 1000 Monte-Carlo simulations using the 'predictive performance evaluation dataset' comprising data from 31 patients after PO single (Fig. 4a) and after PO multiple administration during steady state (Fig. 4b), overlaid with observed data). Whereas predictions of median voriconazole concentrations were in general acceptable after single dosing (Fig. 4a), median concentrations were overpredicted at steady state for models M2 and the aggregate model (Fig. 4b). The 95th percentile at steady state was significantly over- (aggregate model) and underpredicted (M2). The overall best predictive performance at steady state was obtained using model M1 (Fig. 4b, left panel). For all models, graphical evaluation (Fig. S3) and statistical examination (Table S2) of NPDE analysis

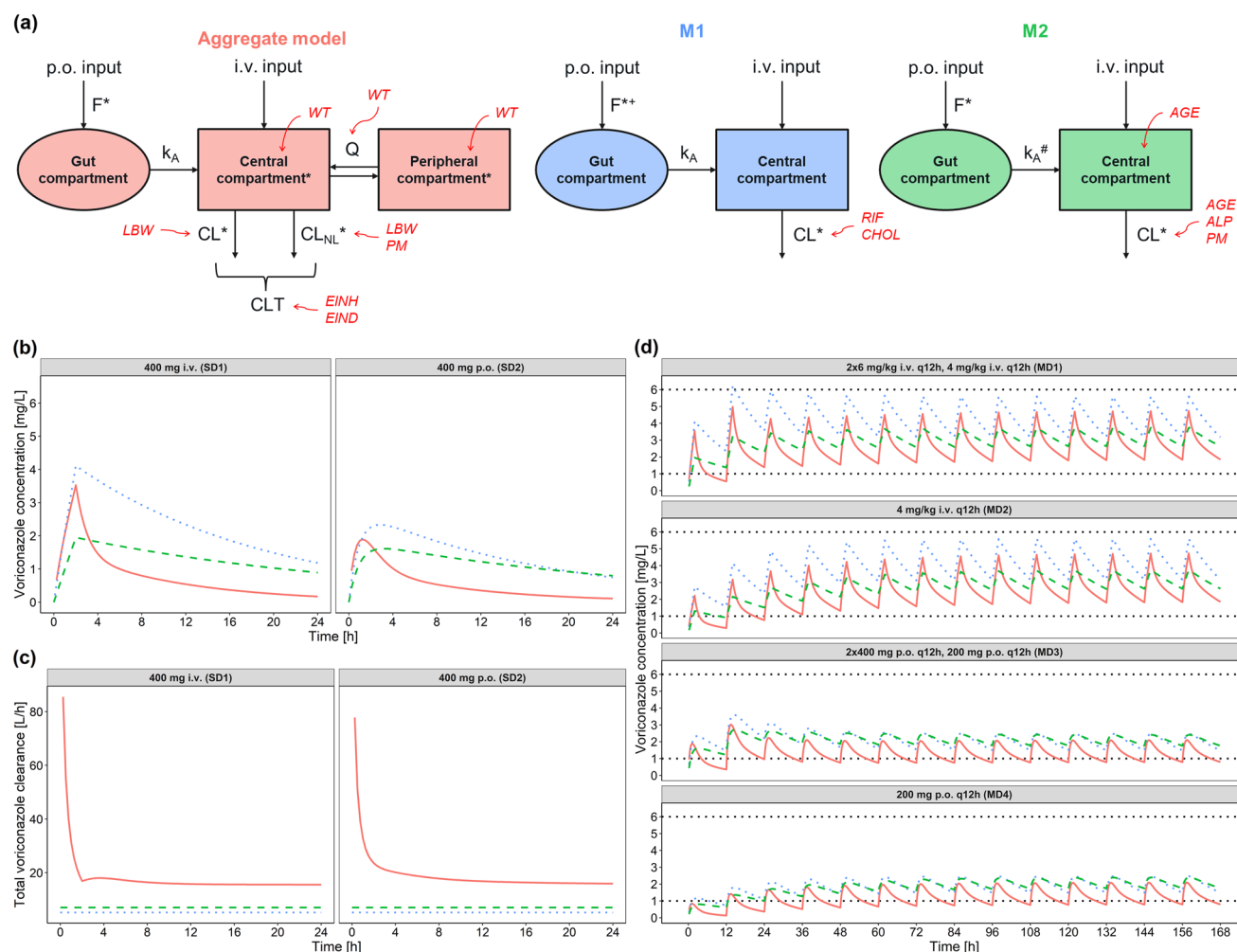


Fig. 2 Identified nonlinear mixed-effects pharmacokinetic models for voriconazole (aggregate model [35], M1 [6] and M2 [13]) (a, upper panel) and deterministic simulations for a 60-year-old, 67 kg typical patient (lean body weight 54 kg) and *CYP2C19**1/*1 genotype (normal metabolizer, wild type), without co-medication using all models (lower panels). Typical voriconazole concentration-time profiles in plasma (b, top lower left panel), and total voriconazole clearance over time (c, bottom lower left panel) after administration of 400 mg voriconazole intravenously over 2 h (400 mg IV, SD1) and 400 mg per orally (400 mg PO, SD2). Typical concentration-time profiles obtained after administration of different multiple IV and PO dosing regimens with (2 × 6 mg/kg IV q12h, then 4 mg/kg IV q12h, MD1, 2 × 400 mg IV q12h, then 200 mg PO q12h, MD3)/without (4 mg/kg IV q12h, MD2, 200 mg PO q12h, MD4) loading doses (d, lower right panels). Solid red line: aggregate model, Dotted blue line: M1, Dashed green line: M2, Dotted black lines (d): lower (1.0 mg/L) and

upper bound (6 mg/L) of C_{min} target range for voriconazole. *Inter-individual variability included on parameter, †Interoccasion variability included on parameter, #Parameter fixed to literature value. *AGE* covariate effect of age, *ALP* covariate effect of alkaline phosphatase, *CHOL* covariate effect of severe hepatic cholestasis, *CL* linear clearance, CL_{NL} time-dependent nonlinear clearance [$V_{max}/(K_M + C_p)$], with V_{max} maximum elimination rate, *CLT* total clearance, C_{min} minimum plasma concentration, C_p plasma concentration, K_M Michaelis-Menten constant, *EIND* covariate effect of enzyme inducer coadministration, *EINH* covariate effect of enzyme inhibitor coadministration, *F* oral bioavailability, *IV* intravenous, k_A absorption rate constant, *LBW* covariate effect of lean body weight (allometric scaling), *PM* covariate effect of *CYP2C19* genotype-predicted phenotype “poor metabolizer”, *PO* per oral, *Q* intercompartmental clearance, *RIF* covariate effect of rifampicin coadministration, *WT* covariate effect of total body weight (allometric scaling)

obtained from 2000 Monte-Carlo simulations showed that the NPDE values were not normally distributed.

The predictive performance in Bayesian forecasting was evaluated in eight individuals using the ‘Bayesian forecasting dataset’ (clinical study design illustrated in Fig. S1). The voriconazole concentration of the 6th occasion was predicted using various numbers and combinations of up

to five previously observed concentrations (workflow illustrated in Fig. S2). Mean prediction error and RMSE were lowest when using all concentrations across all occasions (Fig. 5a, b, pink bar), or, in case of different combinations, when using the ‘latest’ observations (i.e., ‘4’, ‘5’, or ‘4,5’; Fig. 5c, d). When a single sample was utilized, the bias and accuracy of Bayesian forecasting was dependent on the

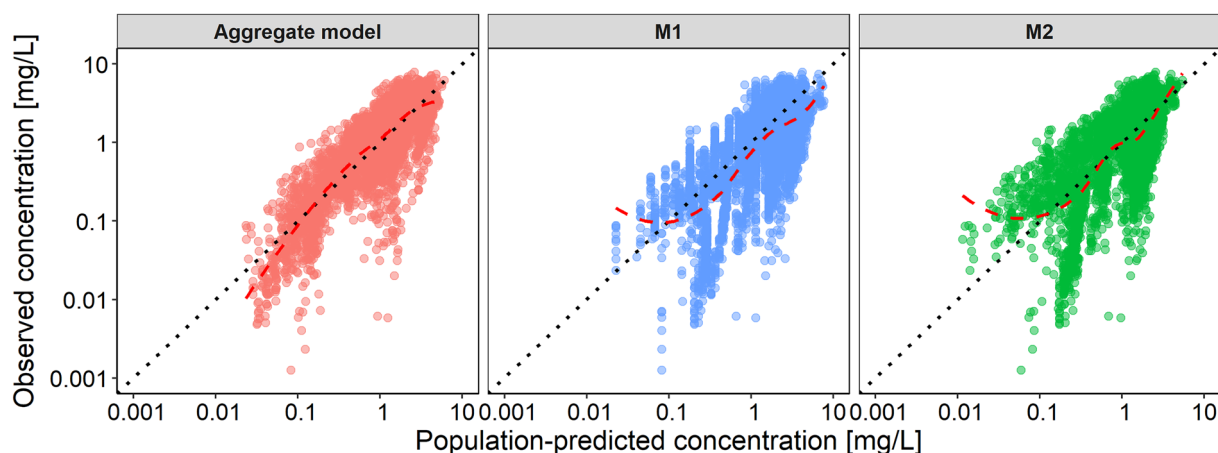


Fig. 3 Population-predicted versus observed voriconazole concentrations using external evaluation dataset stratified by nonlinear mixed-effects pharmacokinetic model of voriconazole. Dotted black line: line of identity, Dashed red line: loess-regression line

Table 3 Population prediction-based results of external model evaluation for the published nonlinear mixed-effects pharmacokinetic models for voriconazole [6, 13, 35]

Characteristic (n_{samples})	Aggregate model		Model 1 (M1)		Model 2 (M2)	
	MPE [%] (95% CI)	RMSE [%]	MPE [%] (95% CI)	RMSE [%]	MPE [%] (95% CI)	RMSE [%]
Overall ($n = 5334$)	36.7 (24.9, 48.4)	438	151 (137, 164)	524	92.5 (81.3, 104)	429
Route of administration						
IV ($n = 2604$)	- 1.73 (- 5.01, 1.56)	85.4	124 (112, 136)	335	40.2 (32.9, 47.4)	192
PO ($n = 2730$)	73.3 (50.7, 95.9)	607	176 (153, 200)	655	142 (122, 163)	569
Population						
Healthy volunteers ($n = 5005$)	30.3 (18.0, 42.5)	443	153 (139, 167)	530	93.0 (81.2, 105)	434
Patients ($n = 329$)	134 (98.2, 169)	354	111 (66.5, 156)	427	85.5 (50.4, 121)	334

All available concentration data were compared to population-predicted concentrations obtained using the respective models in combination with dosing as well as covariate information

95% CI 95% confidence interval, IV intravenous; MPE mean prediction error, PO per oral, RMSE root mean squared error

collection time of the voriconazole concentration relative to the forecasted occasion. Bayesian predicted concentrations were less accurate when obtained using the first ('earliest', Fig. 5c, d, white bar) observed concentration compared with the most recent observed voriconazole concentrations (Fig. 5c, d, red/olive and lilac/pink bars). For both strategies, PEs were displayed over time to investigate the influence on the complete concentration-time profile of the 6th occasion (Fig. S4–S5) and were highest at the beginning and at the end of the dosing interval for all models.

In Figure S6, the population- and individual-predicted concentration-time profiles for strategy a6 (i.e., five prior samples were used to estimate individual PK parameters) were compared to the actual concentration-time profiles of the 6th occasion for a patient with an atypical (815) and with a typical (817) concentration-time profile. Overall, all evaluated models showed only modest predictive performance for the healthy

volunteer and patient populations used in this external evaluation. Across the three candidate models, the aggregate model demonstrated the best predictive performance.

3.3 Clinical Impact of Bayesian Forecasting

A schematic MIPD workflow for voriconazole is proposed in Figure 6a. To illustrate the clinical impact of Bayesian forecasting, the typical concentration-time profile of a virtual patient (based on 'predictive performance evaluation dataset') receiving the standard dosing regimen (MD3) was simulated using the aggregate model (red line; Fig. 6b). Based on a C_{min} sample taken at Day 3 (when $C_{\text{min}} < 1.0$ mg/L), patient-individual PK parameters were estimated, and the trajectory of the concentration-time profile updated (blue line; Fig. 6b). Calculation of individual next dosing regimen showed that increasing the maintenance dosing to 350 mg

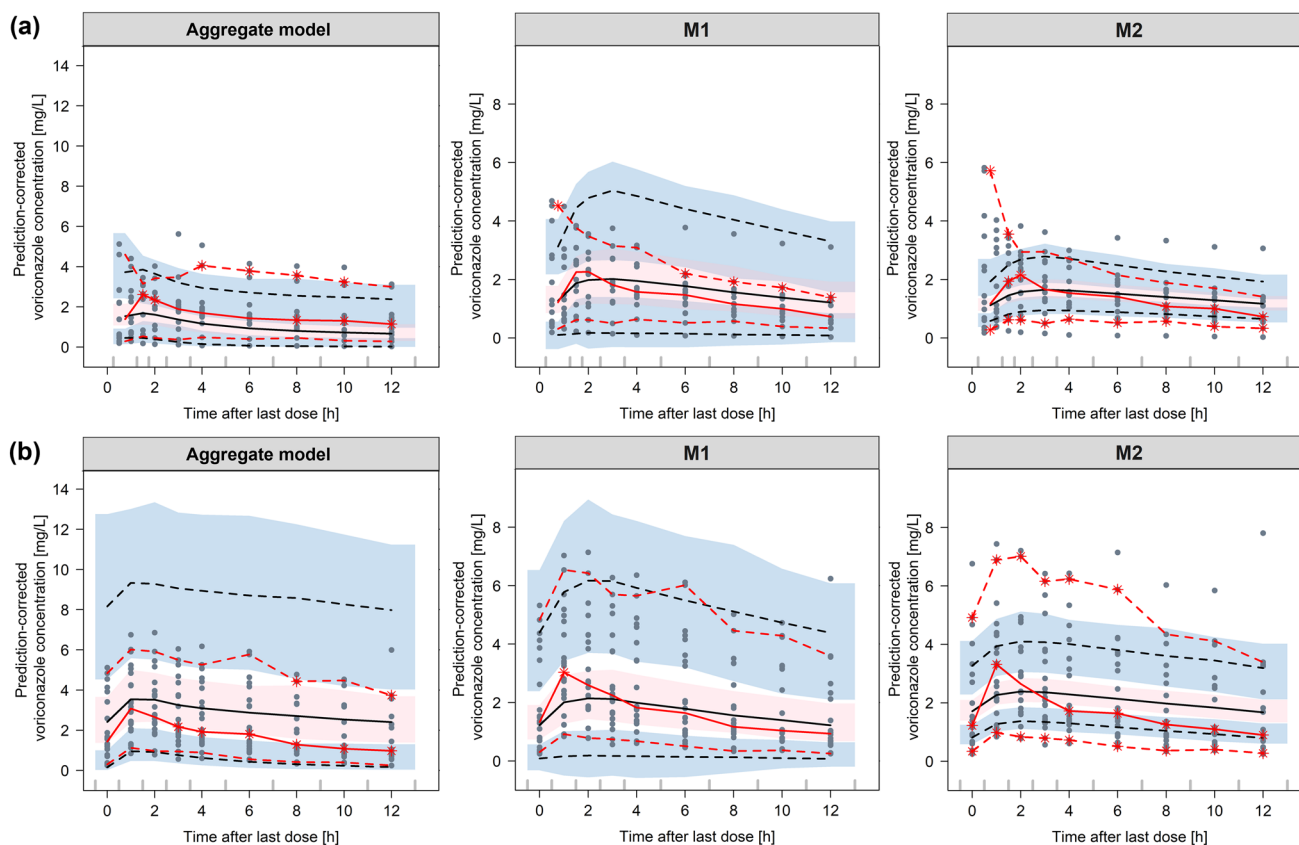


Fig. 4 Prediction-corrected visual predictive checks ($n = 1000$ simulations) using the ‘predictive performance evaluation dataset’ ($n_{\text{samples}} = 329$) comprising data from 31 patients after administration of 400 mg voriconazole (**a**, loading dose, upper panels) and after administration of 200 mg voriconazole at steady state (**b**, maintenance dose, lower panels) stratified by nonlinear mixed-effects pharmacokinetic model of voriconazole. Black circles: observed voriconazole concen-

trations, Lines: 5th, 95th percentile (dashed), 50th percentile (solid) of observed (red) and simulated (black) data, Blue shaded area: 95% CIs around 5th, 95th percentile of simulated data, Red shaded area: 95% CIs around 50th percentile of simulated data, Red stars: percentiles of observed data outside of 95% CIs around percentiles of simulated data

PO q12 h (green line; Fig. 6b) would translate into effective and safe C_{min} for this patient (i.e., reaching the desired C_{min} target range of 1.0–6.0 mg/L).

4 Discussion

Several in silico and clinical studies have shown the benefit of MIPD in supporting and optimizing dosing regimen selection for various drugs [1]. Our study demonstrated the need for thorough external model evaluation before applying a candidate NLME model in the context of MIPD. We identified and selected voriconazole (representative of compounds with complex PK and narrow therapeutic range) as an ideal compound to implement a workflow for model evaluation and MIPD. A published aggregate model for voriconazole comprising features and prior information from six previously published NLME models, was compared with two additional ‘standard’ NLME models. The

aggregate model of voriconazole showed better predictive performance than the ‘standard’ models but overall, the predictive performance of all evaluated models was only modest. This suggests the following knowledge gaps: (i) important PK processes (particularly after PO administration) were not sufficiently implemented in the structural sub-model, (ii) magnitude and sources of interindividual variability were not exhaustively captured, and (iii) interoccasion variability was not adequately accounted for. Our results indicate the need for a comprehensive (pre-)clinical database as basis for NLME model development for MIPD application, to (i) identify and implement critical PK processes in the structural model, (ii) identify sources of interindividual variability, and (iii) adequately quantify interoccasion variability. Successful examples for this (semi-)mechanistic approach comprise rifampicin [53–57], linezolid [58, 59], isoniazid [60], itraconazole [61, 62], and voriconazole [63]. Adequate quantification of

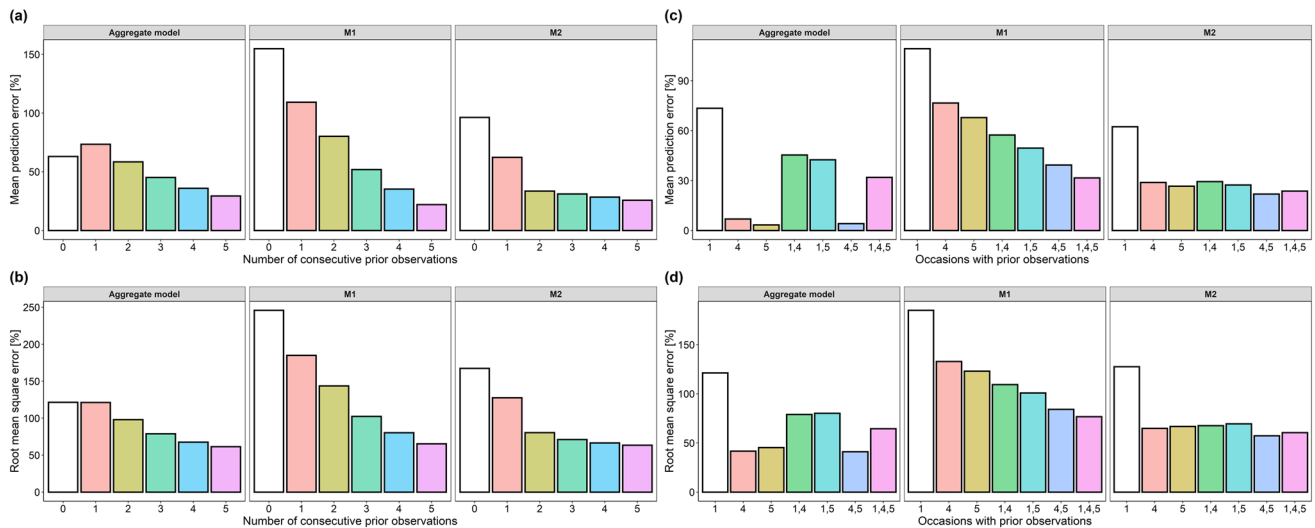


Fig. 5 Relative mean prediction error (**a**, **c**) and relative root mean square error (**b**, **d**) of the predicted versus the observed voriconazole concentrations following the 6th occasion stratified by nonlinear mixed-effects pharmacokinetic model of voriconazole. The individual predicted voriconazole concentrations of the ‘most recent’ (i.e., 6th)

occasion were forecasted by covariate information (a priori prediction) and using the first one, two, three, four, and five prior observations (strategies a1–a6, left panels) or using different combinations of up to three prior observations (strategies b1–b7, right panels)

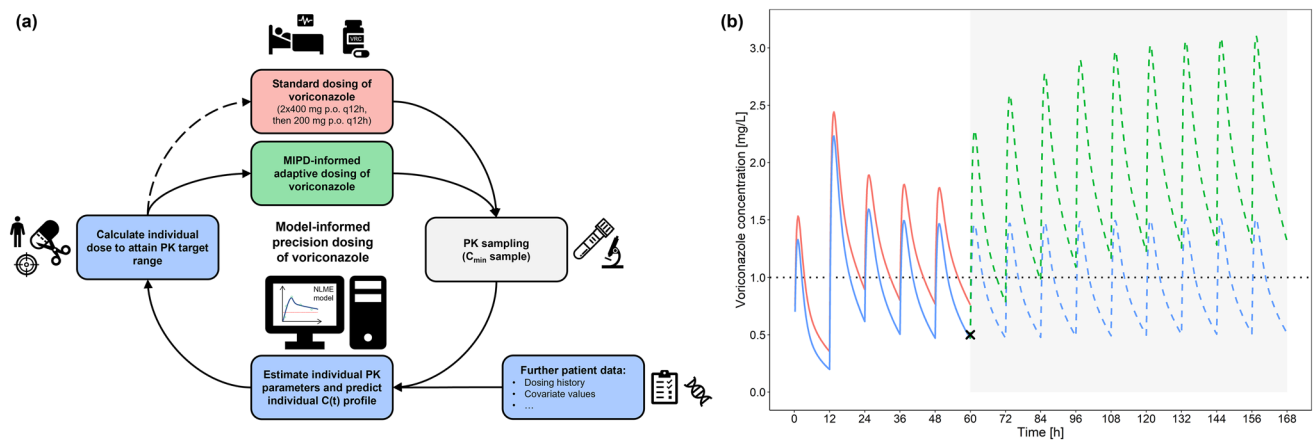


Fig. 6 A schematic model-informed precision dosing workflow for voriconazole (**a**, left panel) and simulation to illustrate the clinical impact of Bayesian forecasting (**b**, right panel). Red line typical: voriconazole concentration-time profile in plasma of a reference patient (based on the characteristics of the ‘predictive performance evaluation dataset’) receiving the standard dosing regimen (MD3) using the aggregate nonlinear mixed-effects pharmacokinetic model of voriconazole, Black cross: C_{\min} sample taken at Day 3, Blue line:

patient-individual concentration-time profile assimilating C_{\min} sample into Bayesian forecast, Green line: updated patient-individual concentration-time profile based on C_{\min} sample and optimized dose of 350 mg, Grey shaded area: indicating future simulation time, Dotted black line: lower bound of C_{\min} target range for voriconazole. C_{\min} minimum plasma concentration, $C(t)$ profile concentration-time profile, MIPD model-informed precision dosing, NLME nonlinear mixed-effects, PK pharmacokinetic(s), PO per oral

interoccasion variability was demonstrated to be an important step for MIPD [39].

Since its approval in the early 2000s, several voriconazole NLME models have been published and reviewed. Voriconazole NLME models are highly variable in structure, including covariates, and parameter values, as the study design, underlying population, and sampling scheme have

a significant impact on the selected model structure. Given the available data, a structural model comprising a lower number of compartments/parameters is often preferred over a more complex (semi-)mechanistic structural model. Consequently, although voriconazole has been characterized as a compound demonstrating complex nonlinear PK [37, 64], inclusion of simple first-order (linear) absorption and

elimination processes was selected for most of the NLME models. Autoinhibition of relevant CYP-mediated elimination pathways, which was determined in vitro [22, 65] and in vivo [21, 66, 67], has only been included in a few NLME models. This process was implemented using an empirical time-dependent function (elimination decreases over time) [68], or an empirical inhibition compartment (elimination decreases with respect to the drug concentration in an empirical inhibition compartment) [69]. Furthermore, significant differences in PK were identified in (i) children and adults, (ii) different *CYP2C19* genotypes and genotype-predicted phenotypes, and (iii) healthy volunteers and patients (mainly due to inflammatory processes) [21, 31]. Most influential covariates identified were age, body size descriptors such as total or lean body weight, liver function markers and co-medication [31]. When available, *CYP2C19* genotype was included primarily as a covariate, such that voriconazole elimination would decrease in the presence of loss-of-function allele *CYP2C19*2* (**1/*2* or **2/*2*). Interestingly, only one NLME model reported a significant influence of gain-of-function allele *CYP2C19*17* on voriconazole clearance [70].

Kallee et al. identified seven population PK models for voriconazole (without pharmacogenetic information) during a systematic literature review [34]. A total of 66 measured voriconazole plasma concentrations from 33 critically ill patients were available for external evaluation. The results indicated that the precision of all models was low, hence the authors concluded that the use of the models is not recommendable and that it should be investigated if models that incorporate pharmacogenetic information would yield better predictive performance. Comparable to our results, the integration of the first TDM sample improved the predictive performance of all models. Huang et al. identified six candidate models for voriconazole suitable for their external evaluation [33]. The published population PK models differed significantly in prediction performance, and none of the models could adequately predict voriconazole concentrations in the external dataset from patients with hematological malignancy. In accordance with findings from our study, Bayesian simulations showed that predictive performance and accuracy of all models were significantly improved when one or two prior concentrations were available.

In our analysis, differences in the ability to accurately predict and forecast voriconazole concentrations were observed between the three investigated NLME models. There was no model demonstrating overall high predictive performance. Implementation of a linear, non-saturable clearance in models M1 and M2 neglected the reported dose dependency and autoinhibition. Voriconazole is almost exclusively eliminated via hepatic metabolism with less than 2% of the dose excreted unchanged in the urine [71]. The activity of metabolizing enzymes can be highly impacted by polymorphisms or co-medication. In the aggregate model,

these mechanisms were accounted for through separation of clearance into two pathways: a constant linear part (representing CYP3A4, CYP2C9 and FMO-mediated metabolism and renal excretion of unchanged drug) and a concentration- and time-dependent nonlinear part (Michaelis-Menten, where V_{\max} is decreasing over time due to CYP2C19-mediated autoinhibition). In a sensitivity analysis, McDougall et al. showed that inclusion of nonlinear clearance was the most important factor for utility of the aggregate model in MIPD [72]. The aggregate model was developed specifically for personalized dosing, and we confirmed the overall best predictive performance. Yet, particularly individual predictions for C_{\min} , were highly variable and forecasted with low precision. All investigated models tended to overestimate observed concentrations, which could lead in the clinical setting to the design of suboptimal dosing regimens resulting in higher risk of treatment failure but lower risk of toxicity. In their recent publications, Wicha et al. identified underlying population size, sampling design, and accurate documentation of dosing and sampling time for model development as main drivers for differences in predictive performance [2, 44, 73].

To our knowledge, the so-called 'hybrid' model approach by McDougall et al. has not yet been systematically evaluated or implemented for other compounds. Other approaches addressing the challenge of selecting the most accurate NLME model as prior for MIPD have been described in the literature. Uster et al. derived an automated model averaging/selection approach to find the best model or combination of models for each patient using vancomycin as a case study [74]. Guo et al. showed that adaptive MAP estimation (which handles data over multiple iterations) outperformed standard MAP-based Bayesian forecasting in predictive performance [75]. Recently, Bayesian data assimilation and reinforcement learning methods were also proposed for MIPD, overcoming major limitations of MAP-based approaches by enabling accurate uncertainty quantification and propagation, and complex patient state/dose combinations, respectively [76–78]. A sequential Bayesian hierarchical modelling framework for continued learning across patients during MIPD (i.e., updating the population parameters using posterior samples) was introduced by Maier et al. using the example of neutrophil-guided dosing of paclitaxel [79]. Hughes et al. demonstrated how a continuous learning approach could be used to adapt a population model to a local environment with a case study in pediatric dosing of vancomycin [80].

To assess the influence of prior observations on model predictivity, different strategies within a Bayesian forecasting setting were investigated. Accuracy and precision of model predictions improved substantially by including voriconazole concentrations using Bayesian forecasting compared to a priori model predictions. In line with

expectations, the most recent voriconazole concentration was found to be the most informative. In our analysis, the “all data” method was used, which bases each forecast on the original prior updated with all concentration data for the individual as it becomes available. Finally, we illustrated an MIPD workflow and demonstrated the clinical impact of Bayesian forecasting for voriconazole (Fig. 6).

Our investigation was primarily limited by the available clinical data, which came mainly from healthy volunteers from two study centers. Due to the very diverse study designs and inclusion of clinical patient data (22.0%), a comprehensive evaluation of voriconazole was still feasible. However, it should be noted that the ‘predictive performance evaluation’ and the ‘Bayesian forecasting’ subsets of the database comprised monocentric data of 31 patients and 8 healthy volunteers, respectively. In some instances, interpretation of the published NLME models was complicated when methodologies were not exhaustively described, and details were missing in the publications. Publication of the full variance-covariance matrix, complete model code, or output files (e.g., *.lst file for NONMEM®) as supplementary materials is highly recommended. In addition, sponsors are highly encouraged to publish the model that was used to analyze the data from pivotal clinical trials (i.e., for the submission), including the clinical trial characteristics.

Despite these limitations, our analysis demonstrates the importance of externally evaluating NLME models before application in the context of MIPD. Our analysis identified a comparatively better model, while confirming the main factors explaining the high interindividual variability. Due to the complex PK of voriconazole, a comprehensive database pooling in vitro and in vivo data from different sources and across multiple clinical studies is needed for development of a more generalizable NLME model. Amalgamating knowledge from translational bottom-up and top-down modelling is a promising approach (‘middle-out’) to elucidate complex PK and to enable development of semi-mechanistic NLME models [22, 81], and has been already successfully applied for other compounds with complex PK, e.g., ciprofloxacin [82, 83], propofol [84], and hydrocortisone [85]. Further inclusion of metabolite data (voriconazole *N*-oxide) in NLME model development and MIPD can improve the assessment of in vivo CYP2C19 activity and thereby prediction of exposure during Bayesian forecasting, especially if the *CYP2C19* genotype of a patient is unknown [86]. The MIPD framework for voriconazole should be expanded in the future by inclusion of saliva PK, pathogen susceptibility and relevant PD markers (specific biomarkers, e.g., galactomannan, or non-specific biomarkers, e.g., C-reactive protein) [87–90].

Carefully designed clinical trials are needed to evaluate the clinical benefit of MIPD [2, 91, 92].

5 Conclusions

This work presents recommendations for evidence-based model development and application of MIPD for compounds with complex PK, illustrated by voriconazole. An aggregate model provided comparatively better predictive performance than two selected ‘standard’ NLME models using external data from a rich in-house clinical database. Ultimately, with further elucidation of the complex PK of voriconazole [21, 22], more (semi-)mechanistic or ‘middle-out’ modelling approaches are warranted for successful implementation of compounds with complex PK in MIPD. Predictive performance of MAP-based MIPD improved using even a single individual concentration, thus at least one PK sample should be obtained. The results of our assessment can guide future implementation of MIPD for voriconazole to improve individual dosing strategies, enhance clinical efficacy, reduce the risk for adverse events, and prevent the spread of antifungal resistance [93].

Supplementary Information The online version contains supplementary material available at <https://doi.org/10.1007/s40262-023-01274-y>.

Declarations

Funding Open Access funding enabled and organized by Projekt DEAL.

Conflict of interest Charlotte Kloft and Wilhelm Huisinga report grants from an industry consortium (AbbVie Deutschland GmbH & Co. K.G., AstraZeneca, Boehringer Ingelheim Pharma GmbH & Co. KG., Gruenthal GmbH, F. Hoffmann-La Roche Ltd., Merck KGaA and Sanofi) for the graduate research training program PharMetriX. In addition, Charlotte Kloft reports research grants from the Innovative Medicines Initiative-Joint Undertaking (“DDMoRe”), from H2020-EU.3.1.3 (“FAIR”), Diurnal Ltd. and the Federal Ministry of Education and Research within the Joint Programming Initiative on Antimicrobial Resistance Initiative (“JPIAMR”), all outside the submitted work. Markus Zeitlinger received grants from Pfizer for other clinical studies, none of them associated with voriconazole. Franziska Kluwe is current employee of Boehringer Ingelheim Pharma GmbH & Co. KG. All other authors declare no competing interests for this work.

Ethics approval All procedures performed in studies involving human participants were in accordance with the ethical standards of the institutional and/or national research committee and with the 1964 Helsinki Declaration and its later amendments or comparable ethical standards. All trial protocols were approved by the responsible Ethics Committees and the respective competent authorities.

Informed consent Written informed consent was obtained from all individual study participants before inclusion.

Availability of data and material The datasets generated during and/or analyzed during the current study are not publicly available as patients did not provide consent for sharing their data in a public database. On reasonable request, the datasets are available from the corresponding author.

Availability of code The NONMEM® code generated during this analysis is available in the electronic supplementary material.

Author contributions Conceptualization: FK, CK; Data collection: MZ, GM, CK; Planning of analysis: FK, RM, GM, CK; Formal analysis and investigation: FK, RM, GM, CK; Writing—original draft preparation: FK, CK; Writing—review and editing: FK, RM, WH, MZ, GM, CK; Supervision: RM, WH, GM, CK. All authors read and approved the final manuscript.

Open Access This article is licensed under a Creative Commons Attribution-NonCommercial 4.0 International License, which permits any non-commercial use, sharing, adaptation, distribution and reproduction in any medium or format, as long as you give appropriate credit to the original author(s) and the source, provide a link to the Creative Commons licence, and indicate if changes were made. The images or other third party material in this article are included in the article's Creative Commons licence, unless indicated otherwise in a credit line to the material. If material is not included in the article's Creative Commons licence and your intended use is not permitted by statutory regulation or exceeds the permitted use, you will need to obtain permission directly from the copyright holder. To view a copy of this licence, visit <http://creativecommons.org/licenses/by-nc/4.0/>.

References

- Kluwe F, Michelet R, Mueller-Schoell A, Maier C, Klopp-Schulze L, Dyk M, et al. Perspectives on model-informed precision dosing in the digital health era: challenges, opportunities, and recommendations. *Clin Pharmacol Ther.* 2021;109:29–36. <https://doi.org/10.1002/cpt.2049>.
- Wicha SG, Märtsen A, Nielsen EI, Koch BCP, Friberg LE, Alffenaar J, et al. From therapeutic drug monitoring to model-informed precision dosing for antibiotics. *Clin Pharmacol Ther.* 2021;109:928–41. <https://doi.org/10.1002/cpt.2202>.
- Darwich AS, Ogungbenro K, Vinks AA, Powell JR, Reny J-L, Marsousi N, et al. Why has model-informed precision dosing not yet become common clinical reality? lessons from the past and a roadmap for the future. *Clin Pharmacol Ther.* 2017;101:646–56. <https://doi.org/10.1002/cpt.659>.
- Donagher J, Martin JH, Barras MA. Individualised medicine: why we need Bayesian dosing. *Intern Med J.* 2017;47:593–600. <https://doi.org/10.1111/imj.13412>.
- World Health Organization (WHO). World Health Organization model list of essential medicines: 22nd list (2021) [Internet]. Geneva PP—Geneva: World Health Organization; 2021. <https://apps.who.int/iris/handle/10665/345533>.
- Pascual A, Csajka C, Buclin T, Bolay S, Bille J, Calandra T, et al. Challenging recommended oral and intravenous voriconazole doses for improved efficacy and safety: population pharmacokinetics-based analysis of adult patients with invasive fungal infections. *Clin Infect Dis.* 2012;55:381–90. <https://doi.org/10.1093/cid/cis437>.
- Luong M-L, Al-Dabbagh M, Groll AH, Racil Z, Nannya Y, Mitsani D, et al. Utility of voriconazole therapeutic drug monitoring: a meta-analysis. *J Antimicrob Chemother.* 2016;71:1786–99. <https://doi.org/10.1093/jac/dkw099>.
- Ashbee HR, Barnes RA, Johnson EM, Richardson MD, Gorton R, Hope WW. Therapeutic drug monitoring (TDM) of antifungal agents: guidelines from the British Society for Medical Mycology. *J Antimicrob Chemother.* 2014;69:1162–76. <https://doi.org/10.1093/jac/dkt508>.
- Pearson MM, Rogers PD, Cleary JD, Chapman SW. Voriconazole: a new triazole antifungal agent. *Ann Pharmacother.* 2003;37:420–32. <https://doi.org/10.1345/aph.1C261>.
- Cordonnier C, Rovira M, Maertens J, Olavarria E, Faucher C, Bilger K, et al. Voriconazole for secondary prophylaxis of invasive fungal infections in allogeneic stem cell transplant recipients: results of the VOSIFI study. *Haematologica.* 2010;95:1762–8. <https://doi.org/10.3324/haematol.2009.020073>.
- Marks DI, Pagliuca A, Kibbler CC, Glasmacher A, Heussel C-P, Kantecki M, et al. Voriconazole versus itraconazole for antifungal prophylaxis following allogeneic haematopoietic stem-cell transplantation. *Br J Haematol.* 2011;155:318–27. <https://doi.org/10.1111/j.1365-2141.2011.08838.x>.
- Jeu L, Piacenti FJ, Lyakhovetskiy AG, Fung HB. Voriconazole. *Clin Ther.* 2003;25:1321–81.
- Wang T, Chen S, Sun J, Cai J, Cheng X, Dong H, et al. Identification of factors influencing the pharmacokinetics of voriconazole and the optimization of dosage regimens based on Monte Carlo simulation in patients with invasive fungal infections. *J Antimicrob Chemother.* 2014;69:463–70. <https://doi.org/10.1093/jac/dkt369>.
- Gautier-Veyret E, Fonrose X, Tonini J, Thiebaut-Bertrand A, Bartoli M, Quesada J-L, et al. Variability of voriconazole plasma concentrations after allogeneic hematopoietic stem cell transplantation: impact of cytochrome P450 polymorphisms and comedication on initial and subsequent trough levels. *Antimicrob Agents Chemother.* 2015;59:2305–14. <https://doi.org/10.1128/AAC.04838-14>.
- Dote S, Sawai M, Nozaki A, Naruhashi K, Kobayashi Y, Nakaniishi H. A retrospective analysis of patient-specific factors on voriconazole clearance. *J Pharm Health Care Sci.* 2016;2:10. <https://doi.org/10.1186/s40780-016-0044-9>.
- Lamoureux F, Duflot T, Woillard J-BB, Metsu D, Pereira T, Compagnon P, et al. Impact of CYP2C19 genetic polymorphisms on voriconazole dosing and exposure in adult patients with invasive fungal infections. *Int J Antimicrob Agents.* 2016;47:124–31. <https://doi.org/10.1016/j.ijantimicag.2015.12.003>.
- Li X, Yu C, Wang T, Chen K, Zhai S, Tang H. Effect of cytochrome P450 2C19 polymorphisms on the clinical outcomes of voriconazole: a systematic review and meta-analysis. *Eur J Clin Pharmacol.* 2016. <https://doi.org/10.1007/s00228-016-2089-y>.
- Veringa A, ter Avest M, Span LFR, van den Heuvel ER, Touw DJ, Zijlstra JG, et al. Voriconazole metabolism is influenced by severe inflammation: a prospective study. *J Antimicrob Chemother.* 2017;72:261–7. <https://doi.org/10.1093/jac/dkw349>.
- Hamadeh IS, Klinker KP, Borgert SJ, Richards AI, Li W, Mangal N, et al. Impact of the CYP2C19 genotype on voriconazole exposure in adults with invasive fungal infections. *Pharmacogenet Genomics.* 2017;450:1. <https://doi.org/10.1097/FPC.0000000000000277>.
- Shao B, Ma Y, Li Q, Wang Y, Zhu Z, Zhao H, et al. Effects of cytochrome P450 3A4 and non-genetic factors on initial voriconazole serum trough concentrations in hematological patients with different cytochrome P450 2C19 genotypes. *Xenobiotica.* 2017;47:1121–9. <https://doi.org/10.1080/00498254.2016.1271960>.
- Schulz J, Kluwe F, Mikus G, Michelet R, Kloft C. Novel insights into the complex pharmacokinetics of voriconazole: a review of its metabolism. *Drug Metab Rev.* 2019;51:247–65. <https://doi.org/10.1080/03602532.2019.1632888>.
- Schulz J, Thomas A, Saleh A, Mikus G, Kloft C, Michelet R. Towards the elucidation of the pharmacokinetics of voriconazole: a quantitative characterization of its metabolism. *Pharmaceutics.* 2022;14:477. <https://doi.org/10.3389/fphar.2020.00283/full>.

23. Schulz J, Michelet R, Zeitlinger M, Mikus G, Kloft C. Microdialysis of drug and drug metabolite: a comprehensive *in vitro* analysis for voriconazole and voriconazole N-oxide. *Pharm Res.* 2022;39:2991–3003. <https://doi.org/10.1007/s11095-022-03292-0>.
24. Schulz J, Michelet R, Zeitlinger M, Mikus G, Kloft C. Microdialysis of voriconazole and its N-oxide metabolite: amalgamating knowledge of distribution and metabolism processes in humans. *Pharm Res.* 2022;39:3279–91. <https://doi.org/10.1007/s11095-022-03407-7>.
25. Purkins L, Wood N, Ghahramani P, Greenhalgh K, Allen MJ, Kleinermaans D. Pharmacokinetics and safety of voriconazole following intravenous- to oral-dose escalation regimens. *Antimicrob Agents Chemother.* 2002;46:2546–53. <https://doi.org/10.1128/AAC.46.8.2546-2553>.
26. Pfizer. VFEND summary of product characteristics. 2018.
27. Johnson LB, Kauffman CA. Voriconazole: a new triazole antifungal agent. *Clin Infect Dis.* 2003;36:630–7. <https://doi.org/10.1086/367933>.
28. Ikeda Y, Umemura K, Kondo K, Sekiguchi K, Miyoshi S, Nakashima M. Pharmacokinetics of voriconazole and cytochrome p450 2C19 genetic status. *Clin Pharmacol Ther.* 2004;75:587–8. <https://doi.org/10.1016/j.clpt.2004.02.002>.
29. Chen K, Zhang X, Ke X, Du G, Yang K, Zhai S. Individualized medication of voriconazole: a practice guideline of the division of therapeutic drug monitoring. *Chinese Pharmacological Society. Ther Drug Monit.* 2018;40:663–74. <https://doi.org/10.1097/FTD.0000000000000561>.
30. Takesue Y, Hanai Y, Oda K, Hamada Y, Ueda T, Mayumi T, et al. Clinical practice guideline for the therapeutic drug monitoring of voriconazole in non-Asian and Asian adult patients: consensus review by the Japanese Society of Chemotherapy and the Japanese Society of Therapeutic Drug Monitoring. *Clin Ther.* 2022;44:1604–23. <https://doi.org/10.1016/j.clinthera.2022.10.005>.
31. Shi C, Xiao Y, Mao Y, Wu J, Lin N. Voriconazole: a review of population pharmacokinetic analyses. *Clin Pharmacokinet.* 2019. <https://doi.org/10.1007/s40262-019-00735-7>.
32. Farkas A, Daroczi G, Villasurda P, Dolton M, Nakagaki M, Roberts JA. Comparative evaluation of the predictive performances of three different structural population pharmacokinetic models to predict future voriconazole concentrations. *Antimicrob Agents Chemother.* 2016;60:6806–12. <https://doi.org/10.1128/AAC.00970-16>.
33. Huang W, Zheng Y, Huang H, Cheng Y, Liu M, Chaphekar N, et al. External evaluation of population pharmacokinetic models for voriconazole in Chinese adult patients with hematological malignancy. *Eur J Clin Pharmacol.* 2022;78:1447–57. <https://doi.org/10.1007/s00228-022-03359-2>.
34. Kallee S, Scharf C, Schatz LM, Paal M, Vogeser M, Irlbeck M, et al. Systematic evaluation of voriconazole pharmacokinetic models without pharmacogenetic information for bayesian forecasting in critically ill patients. *Pharmaceutics.* 2022;14:1920. <https://doi.org/10.3390/pharmaceutics14091920>.
35. McDougall DAJ, Martin J, Playford EG, Green B. Determination of a suitable voriconazole pharmacokinetic model for personalised dosing. *J Pharmacokinet Pharmacodyn.* 2015;43:1–13. <https://doi.org/10.1007/s10928-015-9462-9>.
36. Cheng Y, Wang C, Li Z, Pan Y, Liu M, Jiao Z. Can population pharmacokinetics of antibiotics be extrapolated? Implications of external evaluations. *Clin Pharmacokinet.* 2021;60:53–68. <https://doi.org/10.1007/s40262-020-00937-4>.
37. Kirbs C, Kluwe F, Drescher F, Lackner E, Matzner P, Weiss J, et al. High voriconazole target-site exposure after approved sequence dosing due to nonlinear pharmacokinetics assessed by long-term microdialysis. *Eur J Pharm Sci.* 2019;131:218–29. <https://doi.org/10.1016/j.ejps.2019.02.001>.
38. Abrantes JA, Jönsson S, Karlsson MO, Nielsen EI. Handling interoccasion variability in model-based dose individualization using therapeutic drug monitoring data. *Br J Clin Pharmacol.* 2019;85:1326–36. <https://doi.org/10.1111/bcp.13901>.
39. Keutzer L, Simonsson USH. Individualized dosing with high inter-occasion variability is correctly handled with model-informed precision dosing—using rifampicin as an example. *Front Pharmacol.* 2020;11:1–15. <https://doi.org/10.3389/fphar.2020.00794>.
40. Bergstrand M, Hooker AC, Wallin JE, Karlsson MO. Prediction-corrected visual predictive checks for diagnosing nonlinear mixed-effects models. *AAPS J.* 2011;13:143–51. <https://doi.org/10.1208/s12248-011-9255-z>.
41. Brendel K, Comets E, Laffont C, Mentré F. Evaluation of different tests based on observations for external model evaluation of population analyses. *J Pharmacokinet Pharmacodyn.* 2010;37:49–65. <https://doi.org/10.1007/s10928-009-9143-7>.
42. Nguyen T, Mouksassi M, Holford N, Al-Huniti N, Freedman I, Hooker A, et al. Model evaluation of continuous data pharmacometric models: metrics and graphics. *CPT Pharmacometr Syst Pharmacol.* 2017;6:87–109. <https://doi.org/10.1002/psp4.12161>.
43. Geist MJP, Egerer G, Burhenne J, Riedel K-D, Weiss J, Mikus G. Steady-state pharmacokinetics and metabolism of voriconazole in patients. *J Antimicrob Chemother.* 2013;68:2592–9. <https://doi.org/10.1093/jac/dkt229>.
44. Broecker A, Nardecchia M, Klinker KP, Derendorf H, Day RO, Marriott DJ, et al. Towards precision dosing of vancomycin: a systematic evaluation of pharmacometric models for Bayesian forecasting. *Clin Microbiol Infect.* 2019;25:1286.e1–1286.e7. <https://doi.org/10.1016/j.cmi.2019.02.029>.
45. Katzenmaier S, Markert C, Riedel K-D, Burhenne J, Haefeli WE, Mikus G. Determining the time course of cyp3a inhibition by potent reversible and irreversible CYP3A inhibitors using a limited sampling strategy. *Clin Pharmacol Ther.* 2011;90:666–73. <https://doi.org/10.1038/clpt.2011.164/nature06264>.
46. Bauer RJ. NONMEM tutorial part I: description of commands and options, with simple examples of population analysis. *CPT Pharmacometr Syst Pharmacol.* 2019;8:525–37. <https://doi.org/10.1002/psp4.12404>.
47. Lindbom L, Pihlgren P, Jonsson N. PsN-Toolkit—a collection of computer intensive statistical methods for non-linear mixed effect modeling using NONMEM. *Comput Methods Progr Biomed.* 2005;79:241–57. <https://doi.org/10.1016/j.cmpb.2005.04.005>.
48. Keizer RJ, van Bentem M, Beijnen JH, Schellens JHM, Huitema ADR. Pirana and PCluster: a modeling environment and cluster infrastructure for NONMEM. *Comput Methods Progr Biomed.* 2011;101:72–9. <https://doi.org/10.1016/j.cmpb.2010.04.018>.
49. Jonsson EN, Karlsson MO. Xpose—an S-PLUS based population pharmacokinetic/pharmacodynamic model building aid for NONMEM. *Comput Methods Progr Biomed.* 1998;58:51–64. [https://doi.org/10.1016/s0169-2607\(98\)00067-4](https://doi.org/10.1016/s0169-2607(98)00067-4).
50. Keizer RJ, Karlsson MO, Hooker A. Modeling and simulation workbook for NONMEM: tutorial on Pirana, PsN, and Xpose. *CPT Pharmacometr Syst Pharmacol.* 2013;2:e50. <https://doi.org/10.1038/psp.2013.24>.
51. Elmokadem A, Riggs MM, Baron KT. Quantitative systems pharmacology and physiologically-based pharmacokinetic modeling with mrgsolve: a hands-on tutorial. *CPT Pharmacometr Syst Pharmacol.* 2019;8:883–93. <https://doi.org/10.1002/psp4.12467>.
52. Comets E, Brendel K, Mentré F. Computing normalised prediction distribution errors to evaluate nonlinear mixed-effect models: the npde add-on package for R. *Comput Methods Progr Biomed.* 2008;90:154–66. <https://doi.org/10.1016/j.cmpb.2007.12.002>.

53. Svensson RJ, Niward K, Davies Forsman L, Bruchfeld J, Paues J, Eliasson E, et al. Individualised dosing algorithm and personalised treatment of high-dose rifampicin for tuberculosis. *Br J Clin Pharmacol*. 2019;85:2341–50. <https://doi.org/10.1111/bcp.14048>.
54. Svensson RJ, Aarnoutse RE, Diacon AH, Dawson R, Gillespie SH, Boeree MJ, et al. A population pharmacokinetic model incorporating saturable pharmacokinetics and autoinduction for high rifampicin doses. *Clin Pharmacol Ther*. 2018;103:674–83. <https://doi.org/10.1002/cpt.778>.
55. van Beek SW, ter Heine R, Keizer RJ, Magis-Escurra C, Aarnoutse RE, Svensson EM. Personalized tuberculosis treatment through model-informed dosing of rifampicin. *Clin Pharmacokinet*. 2019;58:815–26. <https://doi.org/10.1007/s40262-018-00732-2>.
56. Svensson E, van der Walt J-S, Barnes KI, Cohen K, Kredt T, Huitema A, et al. Integration of data from multiple sources for simultaneous modelling analysis: experience from nevirapine population pharmacokinetics. *Br J Clin Pharmacol*. 2012;74:465–76. <https://doi.org/10.1111/j.1365-2125.2012.04205.x>.
57. Mikulska MM, Novelli A, Aversa F, Cesaro S, de Rosa FG, Girmenia C, et al. Voriconazole in clinical practice. *J Chemother*. 2012;24:311–27. <https://doi.org/10.1179/1973947812Y.0000000051>.
58. Mockeliunas L, Keutzer L, Sturkenboom MGG, Bolhuis MS, Hulskotte LMG, Akkerman OW, et al. Model-informed precision dosing of linezolid in patients with drug-resistant tuberculosis. *Pharmaceutics*. 2022;14:753. <https://doi.org/10.3390/pharmaceutics14040753>.
59. Plock N, Buerger C, Joukhar C, Kljucar S, Kloft C. Does linezolid inhibit its own metabolism? Population pharmacokinetics as a tool to explain the observed nonlinearity in both healthy volunteers and septic patients. *Drug Metab Dispos*. 2007;35:1816–23. <https://doi.org/10.1124/dmd.106.013755>.
60. van Beek SW, ter Heine R, Alffenaar J-WC, Magis-Escurra C, Aarnoutse RE, Svensson EM, et al. A model-informed method for the purpose of precision dosing of isoniazid in pulmonary tuberculosis. *Clin Pharmacokinet*. 2021;60:943–53. <https://doi.org/10.1007/s40262-020-00971-2>.
61. Abuhelwa AY, Foster DJR, Mudge S, Hayes D, Upton RN. Population pharmacokinetic modeling of itraconazole and hydroxyitraconazole for oral SUBA-itraconazole and sporanox capsule formulations in healthy subjects in fed and fasted states. *Antimicrob Agents Chemother*. 2015;59:5681–96. <https://doi.org/10.1128/AAC.00973-15>.
62. Abuhelwa AY, Mudge S, Upton RN, Foster DJR. Population in vitro-in vivo pharmacokinetic model of first-pass metabolism: itraconazole and hydroxy-itraconazole. *J Pharmacokinetic Pharmacodyn*. 2018;45:181–97. <https://doi.org/10.1007/s10928-017-9555-8>.
63. Li X, Junge L, Taubert M, Georg A Von, Dahlinger D, Starke C, et al. A novel study design using continuous intravenous and intraduodenal infusions of midazolam and voriconazole for mechanistic quantitative assessment of hepatic and intestinal CYP3A inhibition. *J Clin Pharmacol*. 2020;60:1237–53. <https://doi.org/10.1002/jcph.1619>.
64. Theuretzbacher U, Ihle F, Derendorf H. Pharmacokinetic/Pharmacodynamic Profile of Voriconazole. *Clin Pharmacokinet*. 2006;45:649–63. <https://doi.org/10.2165/00003088-200645070-00002>.
65. Jeong S, Nguyen PD, Desta Z. Comprehensive in vitro analysis of voriconazole inhibition of eight cytochrome P450 (CYP) enzymes: major effect on CYPs 2B6, 2C9, 2C19, and 3A. *Antimicrob Agents Chemother*. 2009;53:541–51. <https://doi.org/10.1128/AAC.01123-08>.
66. Hohmann N, Kocheise F, Carls A, Burhenne J, Weiss J, Haefeli WE, et al. Dose-dependent bioavailability and CYP3A inhibition contribute to non-linear pharmacokinetics of voriconazole. *Clin Pharmacokinet*. 2016;55:1535–45. <https://doi.org/10.1007/s40262-016-0416-1>.
67. Hohmann N, Kreuter R, Blank A, Weiss J, Burhenne J, Haefeli WE, et al. Auto-inhibitory properties of the parent but not of the N-oxide metabolite contribute to infusion rate-dependent voriconazole pharmacokinetics. *Br J Clin Pharmacol*. 2017. <https://doi.org/10.1111/bcp.13297>.
68. Friberg LE, Ravva P, Karlsson MO, Liu P. Integrated population pharmacokinetic analysis of voriconazole in children, adolescents, and adults. *Antimicrob Agents Chemother*. 2012;56:3032–42. <https://doi.org/10.1128/AAC.05761-11>.
69. Kim Y, Rhee S, Park WB, Yu K-S, Jang I-J, Lee S. A personalized CYP2C19 phenotype-guided dosing regimen of voriconazole using a population pharmacokinetic analysis. *J Clin Med*. 2019;8:227. <https://doi.org/10.3390/jcm8020227>.
70. Mangal N, Hamadeh IS, Arwood MJ, Cavallari LH, Samant TS, Klinker KP, et al. Optimization of voriconazole therapy for the treatment of invasive fungal infections in adults. *Clin Pharmacol Ther*. 2018;00:1–9. <https://doi.org/10.1002/cpt.1012>.
71. Roffey SJ, Cole S, Comby P, Gibson D, Jezequel SG, Nedderman ANR, et al. The disposition of voriconazole in mouse, rat, rabbit, guinea pig, dog, and human. *Drug Metab Dispos*. 2003;31:731–41. <https://doi.org/10.1124/dmd.31.6.731>.
72. McDougall DAJ, Martin J, Playford EG, Green B. The impact of model-misspecification on model based personalised dosing. *AAPS J*. 2016. <https://doi.org/10.1208/s12248-016-9943-9>.
73. Alihodzic D, Broecker A, Baehr M, Kluge S, Langebrake C, Wicha SG. Impact of inaccurate documentation of sampling and infusion time in model-informed precision dosing. *Front Pharmacol*. 2020;11:1–12. <https://doi.org/10.3389/fphar.2020.00172/full>.
74. Uster DW, Stocker SL, Carland JE, Brett J, Marriott DJE, Day RO, et al. A model averaging/selection approach improves the predictive performance of model-informed precision dosing: vancomycin as a case study. *Clin Pharmacol Ther*. 2021;109:175–83. <https://doi.org/10.1002/cpt.2065>.
75. Guo T, van Hest RM, Zwep LB, Roggeveen LF, Fleuren LM, Bosman RJ, et al. Optimizing predictive performance of Bayesian forecasting for vancomycin concentration in intensive care patients. *Pharm Res*. 2020;37:171. <https://doi.org/10.1007/s11095-020-02908-7>.
76. Maier C, Hartung N, Wiljes J, Kloft C, Huisinga W. Bayesian data assimilation to support informed decision making in individualized chemotherapy. *CPT Pharmacometr Syst Pharmacol*. 2020;9:153–64. <https://doi.org/10.1002/psp4.12492>.
77. Maier C, Hartung N, Kloft C, Huisinga W, Wiljes J. Reinforcement learning and Bayesian data assimilation for model-informed precision dosing in oncology. *CPT Pharmacometr Syst Pharmacol*. 2021;10:241–54. <https://doi.org/10.1002/psp4.12588>.
78. Ribba B, Dudal S, Lavé T, Peck RW. Model-informed artificial intelligence: reinforcement learning for precision dosing. *Clin Pharmacol Ther*. 2020;107:853–7. <https://doi.org/10.1002/cpt.1777>.
79. Maier C, Wiljes J, Hartung N, Kloft C, Huisinga W. A continued learning approach for model-informed precision dosing: updating models in clinical practice. *CPT Pharmacometr Syst Pharmacol*. 2022;11:185–98. <https://doi.org/10.1002/psp4.12745>.
80. Hughes JH, Tong DMH, Lucas SS, Faldasz JD, Goswami S, Keizer RJ. Continuous learning in model-informed precision dosing: a case study in pediatric dosing of vancomycin. *Clin Pharmacol Ther*. 2021;109:233–42. <https://doi.org/10.1002/cpt.2088>.
81. Kluwe F, Schulz J, Huisinga W, Zeitlinger M, Mikus G, Michelet R, et al. Amalgamating knowledge from translational bottom-up and top-down approaches to elucidate complex pharmacokinetics: the voriconazole example. *CPT Pharmacometr Syst Pharmacol*. 2020;9:S14. <https://doi.org/10.1002/psp4.12497>.

82. Schlender J-F, Teutonico D, Coboeken K, Schnizler K, Eissing T, Willmann S, et al. A physiologically-based pharmacokinetic model to describe ciprofloxacin pharmacokinetics over the entire span of life. *Clin Pharmacokinet*. 2018;57:1613–34. <https://doi.org/10.1007/s40262-018-0661-6>.
83. Balbas-Martinez V, Michelet R, Edginton AN, Meesters K, Trocóniz IF, Vermeulen A. Physiologically-based pharmacokinetic model for ciprofloxacin in children with complicated urinary tract infection. *Eur J Pharm Sci*. 2019;128:171–9. <https://doi.org/10.1016/j.ejps.2018.11.033>.
84. Michelet R, Van Bocxlaer J, Allegaert K, Vermeulen A. The use of PBPK modeling across the pediatric age range using propofol as a case. *J Pharmacokinet Pharmacodyn*. 2018;45:765–85. <https://doi.org/10.1007/s10928-018-9607-8>.
85. Michelet R, Bindellini D, Melin J, Neumann U, Blankenstein O, Huisinga W, et al. Insights in the maturational processes influencing hydrocortisone pharmacokinetics in congenital adrenal hyperplasia patients using a middle-out approach. *Front Pharmacol*. 2023. <https://doi.org/10.3389/fphar.2022.1090554/full>.
86. Boglione-Kerrien C, Morcet J, Scaillieux L, Bénézit F, Camus C, Mear J, et al. Contribution of voriconazole N-oxide plasma concentration measurements to voriconazole therapeutic drug monitoring in patients with invasive fungal infection. *Mycoses*. 2023. <https://doi.org/10.1111/myc.13570>.
87. Kim HY, Märtson A-G, Dreesen E, Spriet I, Wicha SG, McLachlan AJ, et al. Saliva for precision dosing of antifungal drugs: saliva population PK model for voriconazole based on a systematic review. *Front Pharmacol*. 2020;11. <https://doi.org/10.3389/fphar.2020.00894>.
88. Vanstraelen K, Maertens J, Augustijns P, Lagrou K, de Loor H, Mols R, et al. Investigation of saliva as an alternative to plasma monitoring of voriconazole. *Clin Pharmacokinet*. 2015;54:1151–60. <https://doi.org/10.1007/s40262-015-0269-z>.
89. Märtson A-G, Alffenaar J-WC, Brüggemann RJ, Hope W. Precision therapy for invasive fungal diseases. *J Fungi*. 2021;8:18. <https://doi.org/10.3390/jof8010018>.
90. van den Born DA, Märtson A-G, Veringa A, Punt NC, van der Werf TS, Alffenaar J-WC, et al. Voriconazole exposure is influenced by inflammation: a population pharmacokinetic model. *Int J Antimicrob Agents*. 2023;61:106750. <https://doi.org/10.1016/j.ijantimicag.2023.106750>.
91. Wright DFB, Martin JH, Cremers S. Spotlight commentary: model-informed precision dosing must demonstrate improved patient outcomes. *Br J Clin Pharmacol*. 2019;85:2238–40. <https://doi.org/10.1111/bcp.14050>.
92. Roggeveen LF, Fleuren LM, Guo T, Thorald P, de Grooth HJ, Swart EL, et al. Right Dose Right Now: bedside data-driven personalized antibiotic dosing in severe sepsis and septic shock—rationale and design of a multicenter randomized controlled superiority trial. *Trials*. 2019;20:745. <https://doi.org/10.1186/s13063-019-3911-5>.
93. Fisher MC, Alastruey-Izquierdo A, Berman J, Bicanic T, Bignell EM, Bowyer P, et al. Tackling the emerging threat of antifungal resistance to human health. *Nat Rev Microbiol*. 2022;20:557–71. <https://doi.org/10.1038/s41579-022-00720-1>.
94. Scholz I, Oberwittler H, Riedel K-D, Burhenne J, Weiss J, Haefeli WE, et al. Pharmacokinetics, metabolism and bioavailability of the triazole antifungal agent voriconazole in relation to CYP2C19 genotype. *Br J Clin Pharmacol*. 2009;68:906–15. <https://doi.org/10.1111/j.1365-2125.2009.03534.x>.
95. Mikus G, Schöwel V, Drzewinska M, Rengelshausen J, Ding R, Riedel K-D, et al. Potent cytochrome P450 2C19 genotype-related interaction between voriconazole and the cytochrome P450 3A4 inhibitor ritonavir. *Clin Pharmacol Ther*. 2006;80:126–35. <https://doi.org/10.1016/j.clpt.2006.04.004>.
96. Rengelshausen J, Banfield M, Riedel K, Burhenne J, Weiss J, Thomsen T, et al. Opposite effects of short-term and long-term St John's wort intake on voriconazole pharmacokinetics. *Clin Pharmacol Ther*. 2005;78:25–33. <https://doi.org/10.1016/j.clpt.2005.01.024>.
97. Nassar YM, Hohmann N, Michelet R, Gottwalt K, Meid AD, Burhenne J, et al. Quantification of the time course of CYP3A inhibition, activation, and induction using a population pharmacokinetic model of microdosed midazolam continuous infusion. *Clin Pharmacokinet*. 2022;61:1595–607. <https://doi.org/10.1007/s40262-022-01175-6>.

Authors and Affiliations

Franziska Kluwe^{1,2}  · Robin Michelet¹  · Wilhelm Huisinga³  · Markus Zeitlinger⁴  · Gerd Mikus^{1,5}  · Charlotte Kloft¹

✉ Charlotte Kloft
charlotte.kloft@fu-berlin.de

Franziska Kluwe
franziska.kluwe@fu-berlin.de

Robin Michelet
robin.michelet@fu-berlin.de

Wilhelm Huisinga
huisinga@uni-potsdam.de

Markus Zeitlinger
markus.zeitlinger@meduniwien.ac.at

Gerd Mikus
gerd.mikus@med.uni-heidelberg.de

¹ Department of Clinical Pharmacy and Biochemistry, Institute of Pharmacy, Freie Universitaet Berlin, Kelchstraße 31, 12169 Berlin, Germany

² Graduate Research Training Program PharMetriX, Berlin/Potsdam, Germany

³ Institute of Mathematics, University of Potsdam, Karl-Liebknecht-Str. 24/25, 14476 Potsdam, Germany

⁴ Department of Clinical Pharmacology, Medical University of Vienna, Waehringer Guertel 18-20, 1090 Vienna, Austria

⁵ Department of Clinical Pharmacology and Pharmacoepidemiology, University Hospital Heidelberg, Im Neuenheimer Feld 419, 69120 Heidelberg, Germany